

Second response theory: A theoretical formalism for the propagation of quantum superpositions

Martín A. Mosquera

Department of Chemistry and Biochemistry, Montana State University, Bozeman, MT 59717, USA

E-mail: martinmosquera@montana.edu

Abstract. The propagation of general electronic quantum states provides information of the interaction of molecular systems with external driving fields. These can also offer understandings regarding non-adiabatic quantum phenomena. Well established methods focus mainly on propagating a quantum system that is initially described exclusively by the ground state wavefunction. In this work, we expand a previously developed size-extensive formalism within coupled cluster theory, called second response theory, so it propagates quantum systems that are initially described by a general linear combination of different states, which can include the ground state, and show how with a special set of time-dependent cluster operators such propagations are performed. Our theory shows strong consistency with numerically exact results for the determination of quantum mechanical observables, probabilities, and coherences. We discuss unperturbed non-stationary states within second response theory and their ability to predict matrix elements that agree with those found in linear and quadratic response theories. This work also discusses an approximate regularized methodology to treat systems with potential instabilities in their ground-state cluster amplitudes, and compares such approximations with respect to reference results from standard unitary theory.

1. Introduction

The quantitative prediction of the behavior of quantum systems is a critical task in electronic structure theory and a main motivator to find improved algorithms and approaches for advanced computing architectures [1–3], such as quantum computers [4–8]. The field of electronic structure has advanced significantly in recent years where it is now possible to perform routinary molecular drug design simulations [9,10], materials high-throughput screening [11,12], simulations of biochemical systems [13,14], among others. In the field of materials research, for instance, localized states in semiconductors that arise from impurities can behave as pseudo-atomic states [15] that are excited by thermal fluctuations or related phenomena. Because of systems like these, a constant target of theory development focuses on computation of energies and forces. However, other properties are also crucial for the engineering of quantum systems [16]. This includes variables such as electrical and magnetic multipolar moments, and their related derivatives. A more advanced type of computation is the direct propagation of a quantum system that involves excited states in its initial state. This is an important goal since non-linear propagations reveal behaviors that are inaccessible by the standard analysis of energetic properties. Real time propagations may also be more computationally efficient than techniques based on eigenvalues/eigenvectors only [17,18], and offer the advantage of being able to capture the response of the system to strong and ultra-strong driving fields, as well as their non-adiabatic couplings to nuclear motion [19].

There is a wide set of electronic structure theories available for different types of applications [20–25]. Among these, coupled cluster (CC) theory is a very reliable formalism to study quantum systems [26–28]. CC methods enjoy the ability to predict accurate quantities that feature size-extensivity [29–32]; meaning they, in principle, scale correctly to the macroscopic scale. They are systematically improvable [33], so they are guaranteed to reach exact numerical values if computational resources allow it. These points have been strong motivators for the scientific community to explore the potential application of CC methods via quantum computers. Unitary CC theory [34–38], for example, has gained significant attention for predicting ground-state energies through quantum algorithms, with promising results [39–42]. Therefore, it can be expected that, as quantum and standard architectures continue to advance, the applicability of CC-based theory and algorithms will expand as well.

Ground-state methods in CC theory have reached a highly productive stage for the design and understanding of molecular systems. Algorithms to study periodic systems have also been deployed recently [43,44]. Excited-state methods, on the other hand, are the subject of on-going theory development. Furthermore, time-dependent (TD) CC formalisms are being designed and implemented to understand quantum systems beyond equilibrium [45–62]. This field started with early theoretical work that explored the potential use of time-dependent CC operators for the calculation of observable quantities in electronic structure and nuclear dynamics [63–67], and it has provided support to such formalisms that continue making progress [46]. These have

made significant advances for propagations that start from the ground state, and in combination with non-Hermitian (standard) CC, variational CC, or unitary CC. There are opportunities, however, to develop formalisms that predict the evolution of general linear combinations of quantum states (which may or may not include the ground state of the system). As common goals with standard CC methods, extended TD techniques must be based on linked diagrammatic expressions and systematic improvability. Quantum superpositions of ground and excited states are fundamental in the study of coherent phenomena. These take place in molecular and materials excitonics, quantum computers, ultracold atoms, quantum spectroscopy, nuclear magnetic and electron paramagnetic resonance experiments, spin lattices, among other physically relevant cases. For these reasons, theoretical techniques capable of predicting time-dependent and frequency-space observable signatures of coherent phenomena are critical. Although we focus in this work on electronic degrees of freedom, the techniques discussed here can be extended to the study of coherent quantum vibrations, or vibronic states.

Motivated by the points above, a TD CC approach was proposed in Ref. [68]. This formalism, called *second response* (SR) theory, can be used to predict the time-dependent behavior of systems that are initially in a linear combination of excited states, while maintaining the desired feature of diagrammatic connectedness (ground states are included through an extra set of equations). We showed the formalism to be consistent with linear and quadratic CC response theories, and validated it successfully with model systems [68]. SR theory is an extension of previous work focused on the linear response of excited states [69–71]. In this work, we show further developments of SR theory in which, by using three TD excitation vectors, the expectation value of a quantum observable as a function of time can be predicted, and this includes probabilities and coherences. Our theory propagates general quantum superpositions that can now include the ground state of the system. We then show the solution of the SR equations that give cluster operators that describe unperturbed non-stationary states. Finally, we discuss an approximated method to treat systems that require regularization to achieve stability. These developments are then verified through a three-electron/three-level system that can be solved exactly using standard unitary quantum propagations.

2. Theory

2.1. Motivation

This work focuses on non-relativistic Coulombic electronic systems. The free (or unperturbed) Hamiltonian, denoted as \hat{H}_0 , is the sum of the kinetic, repulsion, electron-nuclear attraction (assuming fixed nuclei) components. We are interested in electronic systems that are subject to an external perturbation, so the TD Hamiltonian of interest reads $\hat{H}(t) = \hat{H}_0 + \hat{V}(t)$, where $\hat{V}(t)$ is the TD perturbing potential operator. It is important to distinguish two viewpoints: First, standard TD quantum mechanics provides expressions and rules to determine a TD observable of interest. We denote the

initial state of the system in the standard quantum mechanical picture as $\Psi(0)$. Second, our goal is to *develop coupled-cluster equations that propagate the CC analogue of $\Psi(0)$* . So throughout this work we will establish connections between standard quantum mechanical observables and their CC equivalents. For convenience we will often use Heisenberg operators: If \hat{A} denotes the operator corresponding to some observable A of interest, then $\hat{A}^H(t) = \hat{U}^\dagger(t)\hat{A}\hat{U}(t)$, where $\hat{U}(t) = \mathcal{T} \exp[-i \int_0^t \hat{H}(s)ds]$ (with \mathcal{T} denoting the time-ordering superoperator).

We define the *auxiliary wavefunction*:

$$|\Psi_R(t=0; g_R)\rangle = |\Psi_0\rangle + g_R|\Psi(0)\rangle, \quad (1)$$

where:

$$|\Psi(0)\rangle = S|\Psi_0\rangle + \sum_{N \neq 0} C_N |\Psi_N\rangle, \quad (2)$$

Ψ_0 denotes the ground state of the system, g_R a coefficient, and Ψ_N an excited state ($N \neq 0$), the sum (\sum_N) runs over excited states. We also define the wavefunction: $\Psi_E = \sum_{N \neq 0} C_N \Psi_N$. The wavefunctions $\{\Psi_J\}$ satisfy $\hat{H}_0|\Psi_J\rangle = E_J|\Psi_J\rangle$. $\Psi(0)$ is the initial state of interest to be propagated. The exact TD wavefunction of the system reads $|\Psi(t)\rangle = \hat{U}(t)|\Psi(0)\rangle$. If known, $\Psi(t)$ would determine all the measurable quantities of the system. Previous work [68] on SR CC theory showed how to propagate general arbitrary states by computing separately the CC representations of $\langle\Psi_E|\hat{A}^H(t)|\Psi_0\rangle$, and $\langle\Psi_E|\hat{A}^H(t)|\Psi_E\rangle$. In this current work we show how, through an integrated approach, an arbitrary initial state that includes a contribution from the ground state is propagated in SR CC theory. Both approaches are equivalent and give the same numerical results, but the present formulation may offer advantages for potential implementations.

SR theory is motivated by the following property of Ψ_R in standard TD quantum mechanics:

$$\lim_{g_R \rightarrow 0} \frac{\partial}{\partial g_R} |\Psi_R(0; g_R)\rangle = |\Psi(0)\rangle. \quad (3)$$

The derivative with respect to the coefficient g_R is equivalent to the wavefunction $\Psi(0)$, which is a linear combination of quantum states. This combination includes, in principle, any desired number of eigen-states (with $\{C_N\}$ coefficients), which may include the ground-state wavefunction of the system (with S coefficient).

Similarly, we define the conjugate auxiliary wavefunction that depends on a second parameter, g_L :

$$\langle\Psi_L(0; g_L)| = \langle\Psi_0| + g_L\langle\Psi(0)|, \quad (4)$$

which follows $\lim_{g_L \rightarrow 0} \partial/\partial g_L \langle\Psi_L(0; g_L)| = \langle\Psi(0)|$. For CC developments, we denote the operators \hat{X}^J and \hat{T} in terms of the particle-hole excitation operators $\{\hat{\tau}_\mu\}$ (for an excitation labeled μ , when applied to $|0\rangle$, $\hat{\tau}_\mu$ promotes electrons from occupied levels into virtual ones and returns the corresponding wavefunction determinant, [72]), so $\hat{T} = \sum_\mu t_\mu \hat{\tau}_\mu$ and $\hat{X}^J = \sum_\mu X_\mu^J \hat{\tau}_\mu$. \hat{T} is the standard ground-state cluster operator; X_μ^J is defined later below.

Even though the limit procedure is redundant for standard linear combinations, for a CC wavefunction of the form:

$$|\Phi(t=0; g_R)\rangle = \exp \left[\hat{T} + g_R \left(S\hat{X}^0 + \sum_N C_N \hat{X}^N \right) \right] |0\rangle , \quad (5)$$

where $|0\rangle$ is the reference state, it leads to the CC analogue of equation (3), which resembles $\Psi(0)$:

$$\lim_{g_R \rightarrow 0} \frac{\partial}{\partial g_R} |\Phi(t=0; g_R)\rangle = \left(S\hat{X}^0 + \sum_N C_N \hat{X}^N \right) e^{\hat{T}} |0\rangle , \quad (6)$$

where \hat{X}^N is the CC excitation operator from equation-of-motion CC (EOM-CC); \hat{X}^0 is simply the unity in this case [73]. The derivative and limit then yield a linear combination of CC wavefunctions, in analogy with the standard quantum mechanical approach. For instance, the analogue of the eigen-function $|\Psi_N\rangle$ is the CC wavefunction $\hat{X}^N e^{\hat{T}} |0\rangle$. Although these two wavefunctions can in principle lead to the same excited state energies, they are not exactly the same objects, due to the asymmetric (non-Hermitian) nature of standard CC theory [32, 74]. For example, the CC analogue of $\langle \Psi_N |$ is $\langle 0 | \hat{\Lambda}^N \exp(-\hat{T})$, where $\hat{\Lambda}^N$ is the conjugate excitation operator from EOM-CC, and it is expanded as $\hat{\Lambda}^N = \sum_\mu \hat{\tau}_\mu^\dagger \Lambda_\mu^N$. Therefore, the conjugate version is different (not simply a Hermitian conjugate) because the “lambda” vectors must *compensate* for the term $\exp[-\hat{T} - g_R(S\hat{X}^0 + \sum_N C_N \hat{X}^N)]$. Hence we introduce the wavefunction (the CC analogue of $\langle \Psi_L |$):

$$\langle \Upsilon(t=0; g_L, g_R) | = \langle 0 | \hat{\lambda}_m(0; g_L, g_R) \exp[-\hat{x}_m(0; g_R)] , \quad (7)$$

where $\hat{x}_m(0) = \hat{T} + g_R(S\hat{X}^0 + \sum_N C_N \hat{X}^N)$, and $\hat{\lambda}_m = \sum_\mu \hat{\tau}_\mu^\dagger \lambda_{m,\mu}$. Our cluster operator expansions here include an identity term, labeled $\mu = 0$, where $\hat{\tau}_0 = 1$. Due to the non-Hermiticity, the left CC wavefunction has information about the right-handed problem.

Returning to the standard quantum mechanical picture, we consider the expectation value of the auxiliary TD observable $\tilde{A}(t)$:

$$\tilde{A}(t) = \frac{\langle \Psi_L(0) | \hat{A}^H(t) | \Psi_R(0) \rangle}{\mathcal{N}^2} , \quad (8)$$

where $\mathcal{N}^2 = \langle \Psi_L(0) | \Psi_R(0) \rangle = 1 + g_L S^* + g_R S + g_L g_R$. This function satisfies:

$$\begin{aligned} \partial_{LR}^2 \tilde{A}(t) &= \lim_{g_L, g_R \rightarrow 0} \frac{\partial^2}{\partial g_L \partial g_R} \tilde{A}(t) \\ &= \langle \Psi_E | \hat{A}^H(t) | \Psi_E \rangle - (1 - |S|^2) \langle \Psi_0 | \hat{A}^H(t) | \Psi_0 \rangle , \end{aligned} \quad (9)$$

and

$$\begin{aligned} \partial_L \tilde{A}(t) &= \lim_{g_L, g_R \rightarrow 0} \frac{\partial}{\partial g_L} \tilde{A}(t) = \langle \Psi_0 | \hat{A}^H(t) | \Psi_E \rangle , \\ \partial_R \tilde{A}(t) &= \lim_{g_L, g_R \rightarrow 0} \frac{\partial}{\partial g_R} \tilde{A}(t) = \langle \Psi_E | \hat{A}^H(t) | \Psi_0 \rangle . \end{aligned} \quad (10)$$

The last two equations define the operators $\partial_{\text{LR}}^2 = \lim_{g_L, g_R \rightarrow 0} \partial^2 / \partial g_L \partial g_R$, $\partial_L = \lim_{g_L, g_R \rightarrow 0} \partial / \partial g_L$, and $\partial_R = \lim_{g_L, g_R \rightarrow 0} \partial / \partial g_R$. Using these definitions we obtain that the left CC wavefunction must obey:

$$\langle 0 | \left(S^* \hat{L}^0 + \sum_N C_N^* \hat{\Lambda}^N \right) e^{-\hat{T}} = \langle 0 | \partial_L \hat{\lambda}_m(0) e^{-\hat{T}} , \quad (11)$$

giving a term similar to $\langle \Psi(0) |$. We express $\hat{L}_0 = 1 + \hat{\Lambda}$, where $\hat{\Lambda}$ is the “lambda” operator, which is the ground-state left analogue of \hat{T} .

From these two expressions we observe that a TD observable of a system that initiates at a general quantum state, $\Psi(0)$, is obtained (which is a desired result):

$$\langle \Psi(t) | \hat{A} | \Psi(t) \rangle = \partial_{\text{LR}}^2 \tilde{A} + S \partial_L \tilde{A} + S^* \partial_R \tilde{A} + \langle \Psi_0 | \hat{A}^H(t) | \Psi_0 \rangle . \quad (12)$$

In this work, motivated by this relation, we analyze the auxiliary observable \tilde{A} using cluster operators and use the results from such analysis to represent $\langle \Psi(t) | \hat{A} | \Psi(t) \rangle$. In section 6 we apply such expression to study a model 3-level/3-electron system.

2.2. Second response theory

The standard TD equations from CC theory are not limited to propagations from the ground state. For example, using these standard CC equations, one can imagine the situation where a system is driven from the ground-state to another different quantum state. If the simulation were to be restarted at such new quantum state, the system is indeed now being propagated from a state that is not the ground state. However, the evolved “right” excitation TD vector is not connected in a straightforward fashion to the EOM-CC eigen-vectors, nor the conjugate TD excitation vector. This motivates our goal, which is to describe the auxiliary observable shown in equation (8) through CC quantities, then use of the *differential step followed by the limiting procedure* presented in section 2.1 to compute $\langle \Psi(t) | \hat{A} | \Psi(t) \rangle$ (similarly as in Ref. [68]), without calculating the wavefunction $\Psi(t)$ of course. It allows for a connection between EOM-CC eigen-vectors and general TD propagations, where one sets the values of the initial-state coefficients S , and $\{C_N\}$. For this reason, we examine differentiation with respect to the superposition parameters g_L and g_R of the standard CC motion equations:

$$i \partial_t x_{m,\mu}(t) = \langle \hat{\tau}_\mu^\dagger e^{-\hat{x}_m(t)} \hat{H}(t) e^{+\hat{x}_m(t)} \rangle_0 , \quad (13)$$

and

$$-i \partial_t \lambda_{m,\mu}(t) = \langle \hat{\lambda}_m(t) e^{-\hat{x}_m(t)} [\hat{H}(t), \hat{\tau}_\mu] e^{+\hat{x}_m(t)} \rangle_0 , \quad (14)$$

where the subscript “m” indicates the vectors are modified objects as they account for the new initial conditions (which depend on g_L and g_R), $\hat{x}_m = \sum_\mu x_{m,\mu} \hat{\tau}_\mu$, and $\langle \cdot \rangle_0$ denotes average with respect to the reference ($|0\rangle$): $\langle \cdot \rangle_0 = \langle 0 | \cdot | 0 \rangle$. The terms $x_{m,0}$ and $\lambda_{m,0}$ are time-independent (this is a consequence of our TD variational method, [68]). The phase follows the relation: $\partial_t \phi(t) = \langle \hat{\lambda}_m(t) e^{-\hat{x}_m(t)} \hat{H}(t) e^{+\hat{x}_m(t)} \rangle_0$. This number, $\phi(t)$, does not influence the calculation of observable expectation values, so it will not

be considered in detail in this work (its properties are presented in Ref. [68]). These modified operators determine the TD behavior of the following ket and its left conjugate:

$$|\Phi(t; g_R)\rangle = \exp[\hat{x}_m(t) - i\phi(t)]|0\rangle, \quad (15)$$

$$\langle\Upsilon(t; g_R, g_L)| = \langle 0|\hat{\lambda}_m(t) \exp[-\hat{x}_m(t) + i\phi(t)] . \quad (16)$$

The inner product of these two CC wavefunctions is $\langle\Upsilon(t)|\Phi(t)\rangle = \langle\hat{\lambda}_m(t)\rangle_0$.

As shown in Ref. [68], there are four (reduced to three in this work) TD excitation vectors that are needed to compute TD observables. These are: $\hat{x}_r(t) = \partial_R \hat{x}_m(t)$, $\hat{\lambda}_l(t) = \partial_L \hat{\lambda}_m(t)$, $\hat{\lambda}_r(t) = \partial_R \hat{\lambda}_m(t)$, and $\hat{\lambda}_{l,r}(t) = \partial_{LR}^2 \hat{\lambda}_m(t)$. In addition to such vectors, the excitation vectors for a propagation that starts exclusively from the ground state are required as well in our theoretical analysis (for this reason our formalism is called “second response theory”). They are denoted as $\hat{x}(t)$, and $\hat{\lambda}(t)$, so $\hat{x}(0) = \hat{T}$ and $\hat{\lambda}(0) = \hat{L}_0$, and they satisfy equations (13) and (14), respectively. In the limit g_L and g_R tend to zero, $\hat{x}_m(t)$ and $\hat{\lambda}_m(t)$ tend to $\hat{x}(t)$ and $\hat{\lambda}(t)$, respectively. Given the importance of $\lim_{g_R \rightarrow 0} \hat{x}_m(t) = \hat{x}(t)$, we define the quantity:

$$\bar{O}_x(t) = e^{-\hat{x}(t)} \hat{O}(t) e^{+\hat{x}(t)}, \quad (17)$$

where $\hat{O}(t)$ is some observable such as $\hat{H}(t)$ or \hat{A} . The term $\bar{O}_{x,\tau,\mu}(t)$ is used to denote:

$$\bar{O}_{x,\tau,\mu}(t) = [\bar{O}_x(t), \hat{\tau}_\mu], \quad (18)$$

and $\bar{O}_T = e^{-\hat{T}} \hat{O} e^{+\hat{T}}$. The T -transformed free Hamiltonian is denoted as $\bar{H}_T^0 = e^{-\hat{T}} \hat{H}_0 e^{+\hat{T}}$. The Jacobian matrix of EOM-CC is defined as $\mathcal{A}_{\mu\nu} = \langle \hat{\tau}_\mu^\dagger [\bar{H}_T^0, \hat{\tau}_\nu] \rangle_0$. In this way, the vectors \mathbf{X}^J and $\mathbf{\Lambda}^J$ satisfy the equation $\mathcal{A} \mathbf{X}^J = \Omega_J \mathbf{X}^J$ and $(\mathbf{\Lambda}^J)^T \mathcal{A} = (\mathbf{\Lambda}^J)^T \Omega_J$, where $(\mathbf{X}^J)_\mu = X_\mu^J$, $(\mathbf{\Lambda}^J)_\mu = \Lambda_\mu^J$, and Ω_J is the excitation energy (from ground to excited state, $\Omega_J = E_J - E_0$).

Using the operators defined above and based on section 2.1, the initial conditions for the modified vectors are:

$$\hat{x}_m(0; g_R) = \hat{x}(0) + g_R \hat{x}_r(0), \quad (19)$$

and

$$\hat{\lambda}_m(0; g_L, g_R) = \hat{\lambda}(0) + g_L \hat{\lambda}_l(0) + g_R \hat{\lambda}_r(0) + g_L g_R \hat{\lambda}_{l,r}(0), \quad (20)$$

where we will be interested in the limit where g_R and g_L tend to zero, as discussed later on. These limits are necessary to eliminate higher-order terms in powers of g_R and g_L that the modified vectors develop at $t > 0$. As mentioned before, the asymmetric dependencies on g_L and g_R by the excitation operators $\hat{x}_m(t)$ and $\hat{\lambda}_m(t)$ are due to the non-Hermitian attributes of the formalism (these would not take place in unitary CC theory). To elaborate further on this, the vector $\hat{\lambda}_m$ has different features than \hat{x}_m for two reasons: i), the left expression has information about the right-handed problem; hence there must be a vector $\hat{\lambda}_r$. ii), The auxiliary quantum mechanical observable $\tilde{A}(t)$ also depends on the product $g_L g_R$, but the right CC wavefunction is independent of g_L and could not introduce such dependency if \hat{A} were the identity operator. Therefore this dependency on $g_L g_R$ by the CC expression of $\tilde{A}(t)$ requires the term $\hat{\lambda}_{l,r}$, equation (20).

The operators \hat{x}_r , $\hat{\lambda}_l$, $\hat{\lambda}_r$, and $\hat{\lambda}_{l,r}$ follow the relations below [obtained from differentiating the motion equations of \hat{x}_m and $\hat{\lambda}_m$, equations (13) and (14)] [68]:

$$i\partial_t x_{r,\mu}(t) = \langle \hat{\tau}_\mu^\dagger [\bar{H}_x(t), \hat{x}_r(t)] \rangle_0 , \quad (21)$$

$$-i\partial_t \lambda_{l,\mu}(t) = \langle \hat{\lambda}_l(t) [\bar{H}_x(t), \hat{\tau}_\mu] \rangle_0 , \quad (22)$$

$$-i\partial_t \lambda_{r,\mu}(t) = \langle \hat{\lambda}(t) [\bar{H}_{x,\tau,\mu}(t), \hat{x}_r(t)] + \hat{\lambda}_r(t) \bar{H}_{x,\tau,\mu}(t) \rangle_0 , \quad (23)$$

$$-i\partial_t \lambda_{l,r,\mu}(t) = \langle \hat{\lambda}_{l,r}(t) \bar{H}_{x,\tau,\mu}(t) + \hat{\lambda}_l(t) [\bar{H}_{x,\tau,\mu}(t), \hat{x}_r(t)] \rangle_0 . \quad (24)$$

With the equations developed above one can propagate the CC analogue of the state $\Psi(0) = S\Psi_0 + \sum_N C_N \Psi_N$ (or $\Psi(0) = S\Psi_0 + \Psi_E$). This requires that the derivative vectors be expressed in terms of other vectors that ensure solution to equations (21-24) and that initially describe a term like $\langle \Psi(0) | \hat{A} | \Psi(0) \rangle$. First, $\hat{x}_r(t)$ follows the initial condition:

$$\hat{x}_r(0) = S\hat{X}^0 + \sum_N C_N \hat{X}^N , \quad (25)$$

and is propagated as expressed in equation (21). Now, to further simplify the solution of these equations, and generalize Ref. [68] to include a contribution from the ground state, we write

$$\hat{\lambda}_l(t) = \hat{\lambda}_l^E(t) + S^* \hat{\lambda}(t) , \quad (26)$$

where $\hat{\lambda}_l^E(0) = \sum_N C_N^* \hat{\Lambda}^N$, $\hat{\lambda}(0) = \hat{L}_0$, and $t \geq 0$. For the right derivative,

$$\hat{\lambda}_r(t) = \hat{\lambda}_r^E(t) + S \hat{\lambda}(t) , \quad (27)$$

where $\hat{\lambda}_r^E(0) = -\sum_{N,I} C_N F^{NI} \hat{\Lambda}^I / (\Omega_N + \Omega_I)$, $t \geq 0$, and

$$F^{NI} = \sum_{\mu\nu} \langle \hat{L}_0 [[\bar{H}_T^0, \hat{\tau}_\mu], \hat{\tau}_\nu] \rangle_0 X_\mu^N X_\nu^I . \quad (28)$$

For the term $\hat{\lambda}_{l,r}$ we have:

$$\hat{\lambda}_{l,r}(t) = \hat{\lambda}_{l,r}^E(t) + S \hat{\lambda}_l^E(t) + \hat{\lambda}(t) + S^* \hat{\lambda}_r^E(t) , \quad (29)$$

where $\hat{\lambda}_{l,r}^E(t=0) = \sum_J Y^J \hat{\Lambda}^J$, $t \geq 0$, and

$$Y_J = \sum_{N,I} C_N^* C_I \frac{\langle \hat{\Lambda}^N [[\bar{H}_T^0, \hat{X}^J], \hat{X}^I] \rangle_0}{\Omega_N - \Omega_J - \Omega_I} . \quad (30)$$

This expression and that for $\hat{\lambda}_l^E(0)$ are needed for the estimation of the excited-state component of the observable $\hat{A}(t)$ (as shown in section 3). By substituting equations (26-29) into equations (22-24), we observe that $\hat{\lambda}_l^E$, $\hat{\lambda}_r^E$ and $\hat{\lambda}_{l,r}^E$ follow the same equations as $\hat{\lambda}_l$, $\hat{\lambda}_r$ and $\hat{\lambda}_{l,r}$ (supplemental material). Furthermore, these operators simplify the final expression for a TD observable.

We now show that the normalized auxiliary observable below provides excited-state information:

$$\tilde{A}_N(t) = \frac{\langle \Upsilon(t) | \hat{A} | \Phi(t) \rangle}{\mathcal{N}_2^2} , \quad (31)$$

where $\mathcal{N}_2^2 = \langle \Upsilon(t) | \Phi(t) \rangle = 1 + g_L S^* + g_R S + g_L g_R$. The term $\langle \Upsilon(t) | \hat{A} | \Phi(t) \rangle$ is equivalent to $\langle \hat{\lambda}_m(t) \exp[-\hat{x}_m(t)] \hat{A} \exp[+\hat{x}_m(t)] \rangle_0$. This norm is preserved because the relevant scalar amplitudes added to our CC operators do not evolve as a function of time. This auxiliary quantity, \tilde{A}_N , is the CC analogue of the previously defined $\tilde{A}(t)$ TD average.

We observe the following:

$$\begin{aligned} \partial_{LR}^2 \tilde{A}_N(t) &= \langle \hat{\lambda}_l(t) [\bar{A}_x(t), \hat{x}_r(t)] \rangle_0 \\ &\quad - S^* \langle \{ \hat{\lambda}(t) [\bar{A}_x(t), \hat{x}_r(t)] + \hat{\lambda}_r(t) \bar{A}_x(t) \} \rangle_0 \\ &\quad + \langle \{ \hat{\lambda}_{l,r}(t) - S \hat{\lambda}_l(t) \} \bar{A}_x(t) \rangle_0 + (2|S|^2 - 1) \langle \hat{\lambda}(t) \bar{A}_x(t) \rangle_0 , \\ &= \langle \hat{\lambda}_l^E(t) [\bar{A}_x(t), \hat{x}_r(t)] + \hat{\lambda}_{l,r}^E(t) \bar{A}_x(t) \rangle_0 . \end{aligned} \quad (32)$$

We then have that:

$$\begin{aligned} \langle \Psi_E | A^H(t) | \Psi_E \rangle &= \langle \hat{\lambda}_l^E(t) [\bar{A}_x(t), \hat{x}_r(t)] + \hat{\lambda}_{l,r}^E(t) \bar{A}_x(t) \rangle_0 + \\ &\quad (1 - |S|^2) \langle \hat{\lambda}(t) \bar{A}_x(t) \rangle_0 . \end{aligned} \quad (33)$$

The first-order derivatives follow:

$$\partial_L \tilde{A}_N(t) = \langle \hat{\lambda}_l^E(t) \bar{A}_x(t) \rangle_0 , \quad (34)$$

$$\partial_R \tilde{A}_N(t) = \langle \hat{\lambda}_r^E(t) \bar{A}_x(t) + \hat{\lambda}(t) [\bar{A}_x(t), \hat{x}_r(t)] \rangle_0 , \quad (35)$$

so $\langle \Psi_0 | \hat{A}^H(t) | \Psi_E \rangle = \partial_R \tilde{A}_N(t)$ and $\langle \Psi_E | \hat{A}^H(t) | \Psi_0 \rangle = \partial_L \tilde{A}_N(t)$. Combining expressions and using equation (12) we obtain the formula:

$$\langle \Psi(t) | \hat{A} | \Psi(t) \rangle = \langle \hat{\lambda}_l(t) [\bar{A}_x(t), \hat{x}_r(t)] + \hat{\lambda}_{l,r}(t) \bar{A}_x(t) \rangle_0 . \quad (36)$$

We also denote the right hand side of the above equation as $\langle \hat{A} \rangle_{sr}(t)$, with the “sr” subscript implying the average is computed using the SR cluster operators. From this expression we note that in order to predict the evolution of the observable one needs to solve for three TD cluster operators. This equation above is also more compact than that used in Ref. [68], which would require computing matrix elements separately in the case where $S \neq 0$.

The relation shown above, equation (36), is not an exact equality, but a rigorous assignment due to the non-Hermitian nature of the present CC formalism. This aspect is also present in linear and quadratic CC response theories [74]. So a deviation between standard quantum mechanics and the CC formalism is expected to take place, but in our simulations this deviation is small, as discussed later. This is an issue that can be solved by restoring *Hermiticity and unitarity*, where our theoretical foundation remains applicable.

2.3. Determining wavefunction probabilities and coherences

As discussed previously in Ref. [68], the CC wavefunctions do not provide straightforwardly the probability of observing a given eigenstate at a particular point time. In standard wavefunction theory this is accomplished by projecting the eigenstate on the total wavefunction and taking square modulus of the result, *i.e.*, $p_I(t) =$

$|\langle \Psi_I | \Psi(t) \rangle|^2$. As we show in section 6, an alternative to this is to compute such amplitude as a quantum mechanical observable, for example, by defining:

$$\hat{\mathcal{P}}_{IJ} = e^{+\hat{T}} \hat{X}^I |0\rangle \langle 0| \hat{\Lambda}^J e^{-\hat{T}} , \quad (37)$$

which is the CC analogue of $|\Psi_I\rangle\langle\Psi_J|$, setting $\hat{A} = \hat{\mathcal{P}}_{IJ}$, and using equation (36) to compute $p_{IJ}(t)$. More generally, we define $\tilde{p}_{IJ}(t) = \langle \hat{\mathcal{P}}_{IJ} \rangle_{\text{sr}}(t)$ [that is, taking \hat{A} as $\hat{\mathcal{P}}_{IJ}$ in equation (36) and computing accordingly]. The wavefunction-based coherence matrix element $p_{\text{wf},IJ}(t) = C_I^*(t)C_J(t)$ has the evident property: $p_{\text{wf},IJ}^*(t) = p_{\text{wf},JI}(t)$. To satisfy this we compute the coherence as follows:

$$\begin{aligned} \text{Re } p_{IJ}(t) &= \frac{1}{2} [\tilde{p}_{IJ}(t) + \tilde{p}_{JI}(t)] , \\ \text{Im } p_{IJ}(t) &= \frac{1}{2} [\tilde{p}_{IJ}(t) - \tilde{p}_{JI}(t)] . \end{aligned} \quad (38)$$

In section 6 we compare the complex number $p_{IJ}(t)$ to the object $p_{\text{wf},IJ}(t)$ defined above.

3. Unperturbed non-stationary states

In this section we show that well-known matrix elements from linear and quadratic response CC theory can be obtained on the basis of unperturbed SR non-stationary states. We present this development as an example of the consistency of SR theory with respect to LR and QR theory results.

The initial conditions of the excitation vectors can be derived under two considerations: i), The SR theory averages must predict very accurately the exact unitary theory results, and, ii), if the system was originally described by an excited state wavefunction, it should remain in that state when no external perturbation is applied. This is known as a stationary state. Therefore, we need to examine solutions to the set shown in equations (21-24) in absence of perturbations, so $\bar{H}_x(t) = \bar{H}_T^0$. For \hat{x}_r and $\hat{\lambda}_l$, we have that: $\hat{x}_r(t) = \hat{X}^N \exp(-i\Omega_N t)$ and $\hat{\lambda}_l(t) = \hat{\Lambda}^N \exp(+i\Omega_N t)$. These ensure solution to the Jacobian eigenvalue problem: $i\partial_t \mathbf{x}_r = \Omega_N \mathbf{x}_r = \mathcal{A} \mathbf{x}_r$, and $-i\partial_t \boldsymbol{\lambda}_l^T = \Omega_N \boldsymbol{\lambda}_l^T = \boldsymbol{\lambda}_l^T \mathcal{A}$ (where ‘‘T’’ denotes transpose operation).

Now suppose the system is described by a linear superposition of states, leading to an unperturbed non-stationary state, so

$$\hat{x}_r(t) = S\hat{X}^0 + \sum_N C_N \hat{X}^N \exp(-i\Omega_N t) , \quad (39)$$

$$\hat{\lambda}_l(t) = S^* \hat{L}_0 + \sum_N C_N^* \hat{\Lambda}^N \exp(+i\Omega_N t) . \quad (40)$$

With the two solutions above, we can find $\hat{\lambda}_r$ and $\hat{\lambda}_{l,r}$. First, we express $\hat{\lambda}_r(t) = \sum_J d_J(t) \hat{\Lambda}^J + S \hat{L}_0$, where $\{d_J\}$ are TD coefficients (from section 2.2 we note that $\hat{\lambda}(t) = \hat{L}_0$ and $\hat{x}(t) = \hat{T}$ in absence of external perturbations). By using the bi-orthogonality property of the excitation vectors $\{\hat{X}^J, \hat{\Lambda}^J\}$ we observe that

$$-i\partial_t d_J = \sum_N C_N F^{JN} e^{-i\Omega_N t} + \Omega_J d_J(t) , \quad (41)$$

so $d_J(t) = -\sum_N C_N F^{NJ} \exp(-i\Omega_N t)/(\Omega_N + \Omega_J)$. This gives:

$$\hat{\lambda}_r^E(t) = -\sum_{N,J} \frac{F^{NJ}}{\Omega_N + \Omega_J} \hat{\Lambda}^J e^{-i\Omega_N t}, \quad (42)$$

which in turn leads to the TD dependency of $\hat{\lambda}_r$, that is, $\hat{\lambda}_r(t) = \hat{\lambda}_r^E(t) + S\hat{L}_0$. In a similar fashion, if we write $\hat{\lambda}_{l,r}(t) = \sum_J y_J(t)\hat{\Lambda}^J + S\hat{\lambda}_l(t) + \hat{\lambda}(t) + S^*\hat{\lambda}_r^E(t)$, we have that

$$-i\partial_t y_J = \Omega_J y_J(t) + \sum_{M,N} C_M^* C_N \exp[-i(\Omega_N - \Omega_M)t] \langle \hat{\Lambda}^M [[\bar{H}_T^0, \hat{X}^J], \hat{X}^N] \rangle_0, \quad (43)$$

where the sums run over excited states. The solution to the above equation is:

$$y_J(t) = \sum_{M,N} C_M^* C_N \exp[-i(\Omega_N - \Omega_M)t] \frac{\langle \hat{\Lambda}^M [[\bar{H}_T^0, \hat{X}^J], \hat{X}^N] \rangle_0}{\Omega_M - \Omega_J - \Omega_N}. \quad (44)$$

Using the last relation we have that $Y_J = y_J(t=0)$.

The expressions above for perturbation-free evolutions lead to results consistent with linear and quadratic CC response theories. Now, suppose the TD wavefunction is given by $\Psi(t) = \exp(-iE_0 t)[S\Psi_0 + \sum_N C_N \Psi_N \exp(-i\Omega_N t)]$. We note that:

$$\langle \Psi(t) | \hat{A} | \Psi(t) \rangle = |S|^2 \langle \Psi_0 | \hat{A} | \Psi_0 \rangle + \left[S^* \sum_N e^{-i\Omega_N t} \langle \Psi_0 | \hat{A} | \Psi_N \rangle + \text{c.c.} \right] \quad (45)$$

$$+ \sum_{M,N} C_M^* C_N e^{-i(\Omega_N - \Omega_M)t} \langle \Psi_M | \hat{A} | \Psi_N \rangle. \quad (46)$$

Examining the CC analogue of the above equation, based on common phasor terms, we identify the required matrix elements. These are, the term

$$\langle \Psi_N | \hat{A} | \Psi_0 \rangle = \langle \hat{\Lambda}^N \bar{A}_T \rangle_0, \quad (47)$$

its conjugate:

$$\langle \Psi_0 | \hat{A} | \Psi_N \rangle = \langle \hat{L}_0 [\bar{A}_T, \hat{X}^N] \rangle_0 - \sum_J \frac{F^{NJ}}{\Omega_J + \Omega_N} \langle \hat{\Lambda}^J \bar{A}_T \rangle_0, \quad (48)$$

and the excited-state/excited-state element:

$$\langle \Psi_M | \hat{A} | \Psi_N \rangle = \delta_{MN} \langle \hat{L}_0 \bar{A}_T \rangle_0 + \langle \hat{\Lambda}^M [\bar{A}_T, \hat{X}^N] \rangle_0 \quad (49)$$

$$+ \sum_J \frac{\langle \hat{\Lambda}^M [[\bar{H}_T^0, \hat{X}^J], \hat{X}^N] \rangle_0}{\Omega_M - \Omega_J - \Omega_N} \langle \hat{\Lambda}^J \bar{A}_T \rangle_0. \quad (50)$$

Equations (47) and (48) are identical to those from CC linear response theory, and equation (50) was derived originally within the context of CC quadratic response theory [32]. These equations clearly illustrate the non-Hermiticity of the present formalism, where interchanging labels ($N \leftrightarrow M$, for example) gives different formulas [74].

4. Approximated scheme based on regularization

Even though standard CC theory is designed to address dynamically correlated systems, or more challenging cases through spin symmetry breaking, there can be scenarios where solving the CC equations is difficult due to low-energy gaps or related instabilities in the numerical solution methods used to determine $\{t_\mu\}$ (these can occur in perturbation theory applications [75, 76]). The CC variational method is not necessarily restricted in use to non-relativistic Coulombic Hamiltonians, but it can also be applied to double-hybrid DFT Hamiltonians, and model systems such as those described by Hubbard Hamiltonians (or similar), where this issue may occur. To circumvent numerical instabilities (*i.e.*, divergences in $\{t_\mu\}$) when they take place and facilitate the determination of a wavefunction of the form $\exp(\hat{T})|0\rangle$, regularization can be an appealing approach. It may not provide a completely physically meaningful wavefunction in some cases, but such wavefunction could be used as a starting point for alternative formalisms that could need it. In the context of DFT, we showed for the dissociation of fundamental diatomic molecules that regularization can eliminate instabilities and give results with consistent physical meaning [77].

As we proposed it previously [78], one can regularize the equations by adding an additional term, and find the stationary point of the function (inspired from the standard variational method [79, 80]):

$$\mathcal{E}(\alpha) = \text{stat.}_{\mathbf{\Lambda}, \mathbf{t}} \left[\langle (1 + \hat{\Lambda}) e^{-\hat{T}} \hat{H}_0 e^{+\hat{T}} \rangle_0 + \alpha \mathbf{\Lambda} \cdot \mathbf{t} \right], \quad (51)$$

where α is a regularization number, $\mathbf{\Lambda} \cdot \mathbf{t} = \sum_\mu \Lambda_\mu t_\mu$, and “stat.” stands for stationarization (the minimization principle does not apply to this case). We denote the solution to the problem above as $\{\Lambda'_\mu\}$ and $\{t'_\mu\}$ (the prime symbol indicating these are regularized solutions). We also define $\hat{L}' = 1 + \hat{\Lambda}'$. In this section we focus on the eigen-value problem.

We wish to apply the SR method in this case for $t = 0$ only. With the solution regularized, the wavefunction Ψ_R takes a different form, where the term that is not multiplied by g_R is a reference state that is the standard quantum mechanical analogue of $\exp(\hat{T}')|0\rangle$ (which is not the true ground state CC wavefunction). If we denote this wavefunction as Ψ'_0 , then $|\Psi_R(0, g_R)\rangle = |\Psi'_0\rangle + g_R|\Psi(0)\rangle$, where $\Psi(0)$ is a state we want to represent using a CC object, such as the true ground state or an excited state of interest. The CC wavefunctions that we seek here are of the form $\hat{X}^N \exp(\hat{T}')|0\rangle$ and $\langle 0| \exp(-\hat{T}') \hat{\Lambda}^N$. So we take $\hat{x}(0) = \hat{T}'$ and $\lambda(0) = \hat{L}'$.

For $\hat{A} = \hat{H}_0$, we then have, from equation (36), the approximation:

$$E = \langle \hat{\Lambda} [\bar{H}_{T'}^0, \hat{X}] \rangle_0 + \langle \hat{L}' \bar{H}_{T'}^0 \rangle_0, \quad (52)$$

where E represents $\langle \Psi(0) | \hat{H} | \Psi(0) \rangle$, and $\bar{H}_{T'}^0 = e^{-\hat{T}'} \hat{H}_0 e^{+\hat{T}'}$. We treat \hat{X} and $\hat{\Lambda}$ as variational quantities. We also define $\tilde{\mathcal{A}}_{\mu\nu} = \langle \hat{\tau}_\mu^\dagger [\bar{H}_{T'}, \hat{\tau}_\nu] \rangle_0$, which is now based on the regularized Hamiltonian. Note that the identity operator $\hat{\tau}_0 = 1$ is not required to expand the excitation operators (\hat{X} and $\hat{\Lambda}$) because it commutes with $\bar{H}_{T'}$ (but in a different formulation including $\hat{\tau}_0$ may be necessary).

With these definitions we have:

$$E = (\mathbf{\Lambda})^T \tilde{\mathbf{A}} \mathbf{X} + \langle \hat{L}' \bar{H}_{T'}^0 \rangle_0, \quad (53)$$

and the eigenvalue problem takes the form: $(\mathbf{\Lambda}^N)^T \tilde{\mathbf{A}} = (\mathbf{\Lambda}^N)^T \tilde{\Omega}_N$ and $\tilde{\mathbf{A}} \mathbf{X}^N = \tilde{\Omega}_N \mathbf{X}^N$, where $\tilde{\Omega}_I = E_I - E'_0$ and $E'_0 = \langle \hat{L}' \bar{H}_{T'}^0 \rangle_0$. The estimated energies of interest are then $E_I = \tilde{\Omega}_I + E'_0$. As expected, by solving this problem one also obtains approximated values for the excited-state energies $\{E_I\}$, $I \neq 0$.

Assuming that $\hat{\lambda}(0) = \hat{L}'$ renders the present method as approximated in essence. It can be shown that in a more rigorous approach $\hat{\lambda}(0)$ involves more terms, but this requires a careful response theory analysis that includes the fact that $\exp(\hat{T}')|0\rangle$ is a linear combination of the eigen-states of the Hamiltonian \hat{H}_0 , which is beyond the current scope.

5. Computational methodology

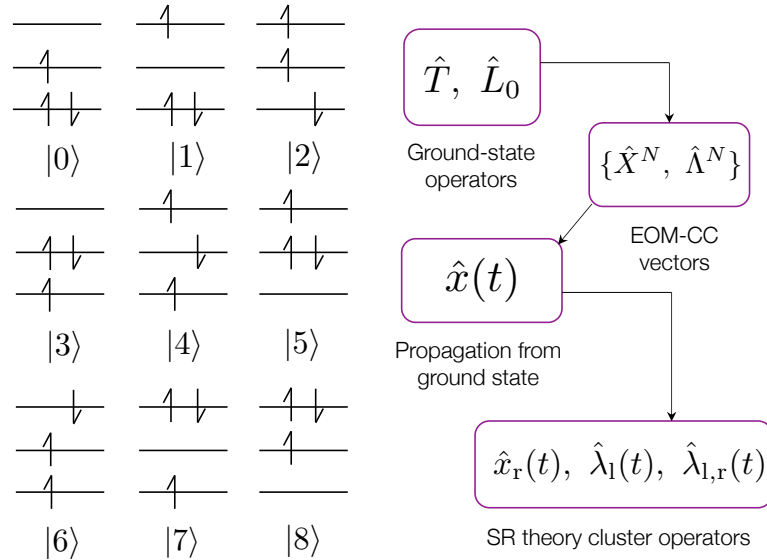


Figure 1. Electronic configurations used (left), and operators needed to compute properties arising from propagations that start from a quantum linear superposition (right). A quantum mechanical TD average is then computed using the vectors shown in this figure, and equation (36). The reference is the state $|0\rangle$.

To explore the SR CC theoretical propagation method developed in this work, we examine a three-level/three-electron system. In the reference configuration $|0\rangle$, the first energy level, labeled “ j ”, is doubly occupied, the next level, “ i ”, is singly occupied, and the virtual level, “ a ”, is unoccupied. We consider a non-trivial Hamiltonian that features two-electron interactions, and a strong driving perturbation. The unperturbed Hamiltonian has the form:

$$\hat{H}_0 = \hat{h}_0 + \sum_q U_q \hat{n}_{q\uparrow} \hat{n}_{q\downarrow} + \left[\sum_{\mu > \nu} W_{\mu\nu} \hat{\tau}_\mu \hat{\tau}_\nu + \text{H.c.} \right], \quad (54)$$

where the single particle Hamiltonian, \hat{h}_0 , reads: $\hat{h}_0 = \sum_p \epsilon_p \hat{n}_p + \sum_\mu b_\mu [\hat{\tau}_\mu + \hat{\tau}_\mu^\dagger]$. The number operator for a spin-level reads $\hat{n}_{q\sigma} = \hat{q}_\sigma^\dagger \hat{q}_\sigma$, and $\hat{n}_p = \hat{n}_{p\downarrow} + \hat{n}_{p\uparrow}$ is the number operator of level p . We take $b_\mu = b$, $W_{\mu\nu} = w_0$, $U_a = U_i = U_0$, and $U_j = 0$. All the single-particle orbital levels are equally spaced by a $\Delta\epsilon$ term, and we also set $\epsilon_j = 0$ for convenience.

Having defined the free Hamiltonian of the system, the full TD energy operator is defined as:

$$\hat{H}(t) = \hat{H}_0 - f(t)\hat{D}. \quad (55)$$

In this case we take the dipole operator as $\hat{D} = d_0 \sum_\mu [\hat{\tau}_\mu + \hat{\tau}_\mu^\dagger]$, and the driving function corresponds to a rectangular pulse of the form $f(t) = f_0$ if $0 < t < t_0$ ($t_0 = 5$ fs), $f(t) = 0$, otherwise.

In section 6 we propagate standard and CC-based quantum superpositions and compare the results. We then show that the regularized scheme leads to consistent results with respect to both the reference and the SR CC results. For these numerical simulations we assume that $\Delta\epsilon = 1$ eV, $\epsilon_j = 0$, $\epsilon_i = \Delta\epsilon$, and $\epsilon_a = 2\Delta\epsilon$. We take $b = 0.1$ eV, $w_0 = U_0 = 0.2$ eV, $d_0 = 0.5$, and $f_0 = 0.04$ au (or 2.1×10^{10} V/m); other values are specified accordingly in section 6. Figure 1 shows a basic schematics of the three-electron/three-level system of interest in terms of its single-particle basis. There are nine configurations that lead to nine full-body wavefunctions.

In physical terms, an $M_s = +1/2$ system with equally “spaced” energy levels, initially in a linear combination of states, is subject to an external perturbation. We use our SR CC method to compute expectation values and compare against numerically exact standard (unitary) quantum mechanics. In figure 1 we show the steps required to perform a propagation based on SR theory. First, one solves the ground- and excited-state CC problems, which give the operators \hat{T} , $\hat{\Lambda}$, $\{\hat{X}^N\}$, and $\{\hat{\Lambda}^N\}$. Then one determines the operator $\hat{x}(t)$, through solution of the standard TD CC equations that propagate a system that initiates at the ground-state. Following this step, one solves the SR TD relations, equations (21, 22, and 24), for \hat{x}_r , $\hat{\lambda}_l$, and $\hat{\lambda}_{l,r}$, and uses these vectors in equation (36) to compute the TD observable A . The initial conditions are applied as well, as discussed in section 2.2, and which are based on the S , and $\{C_N\}$ coefficients. To solve the TD SR equations, we use the midpoint method (or second order Runge-Kutta technique) in the range $[0 - 50$ fs]; this is based on 50,000 steps.

6. Results and discussion

The standard eigenstates of the system are obtained by diagonalizing the unperturbed Hamiltonian, such that $\hat{H}_0|\Psi_J\rangle = E_J|\Psi_J\rangle$, $J = 0, 1, \dots, 8$ (details about these states can be found in the supplemental material). In an analogous fashion, we first solve the ground-state CC problem iteratively to find \hat{T} and $\hat{\Lambda}$, then the left and right eigenvalue problems (with matrix \mathcal{A}) are solved to determine the set $\{\mathbf{\Lambda}^I, \mathbf{X}^I\}$ ($I = 1, \dots, 8$). Having these eigenvalue problems solved, in order to generate reference quantum

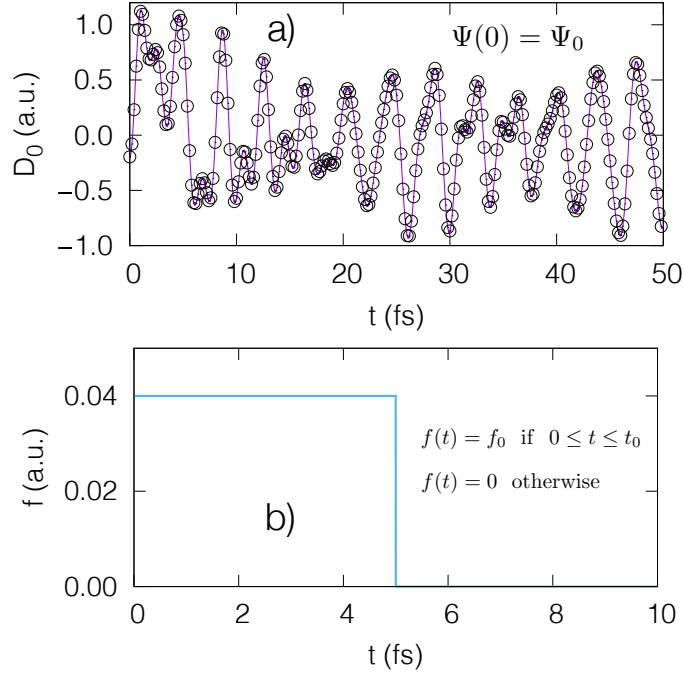


Figure 2. Standard propagation and driving pulse. a), Time-dependent dipole, $D_0(t) = \langle \Psi_0 | \hat{D}^H(t) | \Psi_0 \rangle$, for propagation from the ground-state of the system: open circles denote the standard TD CC propagation, purple line refers to the unitary reference result (numerically exact). b), Shape of the pulse applied (shown between 0 and 10 fs), which is turned-off at $t = 5$ fs.

mechanical data, we proceed to propagate the standard wavefunction of the system using $i\partial_t \Psi(t) = \hat{H}(t)\Psi(t)$ [as $\Psi(t+\delta t) = \exp\{-i\delta t \hat{H}(t+\delta t/2)\}\Psi(t)$]. Then, we solve the second response equations for $\hat{\lambda}_l$, $\hat{\lambda}_{l,r}$, and \hat{x}_r , equations (21, 22, and 24), as mentioned in section 5. The TD observable is computed for both cases using $\langle \Psi(0) | \hat{A}^H(t) | \Psi(0) \rangle$ (which serves as reference) and $\langle \hat{\lambda}_l(t) [\bar{A}_x(t), \hat{x}_r(t)] + \hat{\lambda}_{l,r}(t) \bar{A}_x(t) \rangle_0$. We study the propagation of three different initial states, denoted “QS1”, “QS2”, and “QS3”, respectively (“QS” standing for “quantum superposition”). These initial states are defined as follows:

$$\text{QS1: } \Psi(0) = \frac{1}{\sqrt{3}}\Psi_0 + \frac{1}{\sqrt{3}}\Psi_1 + \frac{1}{\sqrt{3}}\Psi_2, \quad (56)$$

$$\text{QS2: } \Psi(0) = \frac{1}{\sqrt{2}}\Psi_7 + \frac{i}{\sqrt{2}}\Psi_8, \quad (57)$$

$$\text{QS3: } \Psi(0) = \frac{1}{\sqrt{4}}\Psi_0 + \frac{1}{\sqrt{4}}\Psi_3 + \frac{1}{\sqrt{2}}\Psi_5. \quad (58)$$

Note that QS2 features a complex-valued coefficient ($C_8 = i/\sqrt{2}$).

The Hamiltonian \hat{H}_0 yields a ground state that is non-trivial, where the contributions of the singles and doubles configurations are in the range $[0.04 - 0.1]$. These are significant contributions to the reference of the system. Figure 2.a shows the result of propagating the *ground-state* using the standard unitary and the CC methods. As expected, the TD standard CC equations reproduce quite well the unitary results. As mentioned before, from this propagation one needs the vector $\hat{x}(t)$ to

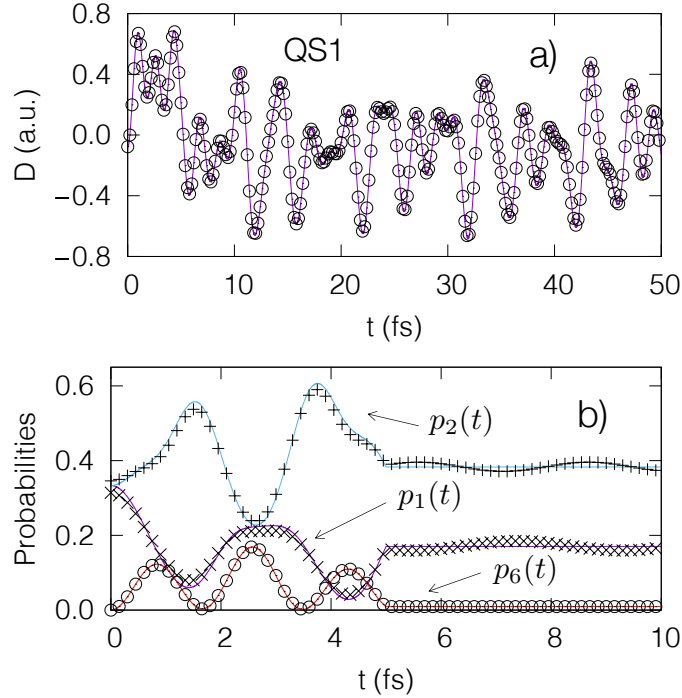


Figure 3. Evolution of the system as initiating in the QS1 state in terms of the dipole and probabilities, $D(t) = \langle \text{QS1} | \hat{D}^H(t) | \text{QS1} \rangle$, where $|\text{QS1}\rangle$ denotes the first initial quantum superposition shown in equation (56). a), TD dipole: purple line corresponds to the numerically exact unitary result, open circles denote the SR CC theory results. b), Probabilities of the unperturbed Hamiltonian eigenstates Ψ_1 (purple line: exact result, cross symbol: SR theory), Ψ_2 (blue line: exact result, “+” symbol: SR theory), and Ψ_6 (red line: unitary simulation, open circle: SR theory).

propagate quantum superpositions; the operator $\hat{\lambda}(t)$ is not needed as $\hat{\lambda}_{l,r}(t)$ contains the information about this cluster operator. To illustrate the applicability of the SR method, we begin considering the initial state “QS1”, $\Psi(0) = C_0\Psi_0 + C_1\Psi_1 + C_2\Psi_2$, where $C_0 = C_1 = C_2 = 1/\sqrt{3}$ (also note that $S = C_0$). The state Ψ_0 is dominated by the reference configuration ($|0\rangle$), Ψ_1 by the first configuration ($|1\rangle$), and Ψ_2 by the third configuration ($|3\rangle$); this also applies to the their corresponding EOM-CC eigenstates. Figure 3.a displays the comparison between the standard unitary and SR theory propagations for the dipole, and figure 3.b the eigenstate probabilities. The agreement between these two propagations is noticeable. Our propagations are entirely coherent due to the absence of dissipative effects. For this reason, after the perturbation is turned off, the dipole remains oscillating. The exact probabilities, as expected, reach a steady value after $t = 5$ fs. The estimates obtained from the CC operator $\hat{\mathcal{P}}_{II}$, except $p_6(t)$, however, show relatively small deviations after 5 fs. The use of this operator, nonetheless, yields a more desirable consistency than the other estimators discussed previously in Ref. [68]. We attribute this again to the asymmetric characteristics of the formalism and the truncation (up to the fourth order) of $\exp[-\hat{x}(t)]\hat{\mathcal{P}}_{IJ}\exp[\hat{x}(t)]$. Figure 4 displays the TD evolution of the populations of the levels i and a , where a

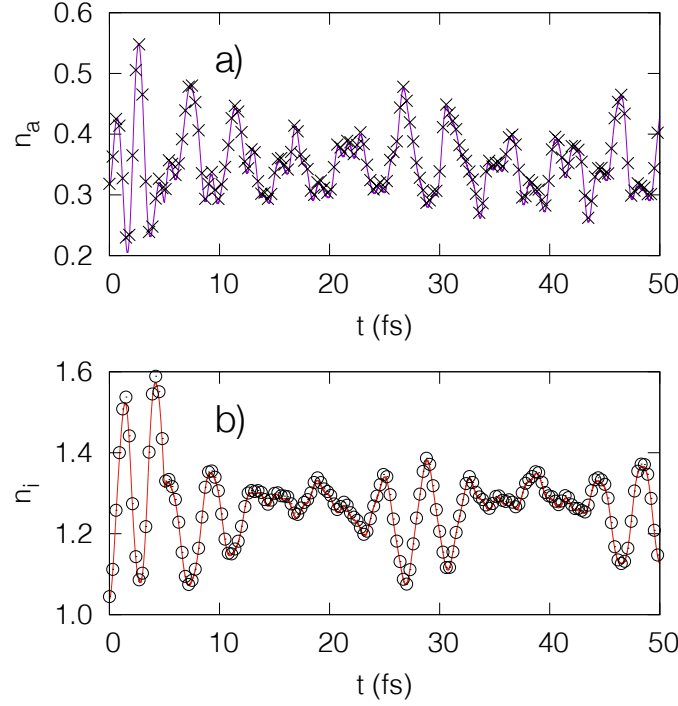


Figure 4. a), TD population of level a , purple line: exact result, cross symbols: SR theory. b), TD population of level i , red line: unitary simulation, open circles: SR CC theory.

better overall agreement is observed in comparison to the eigenstate probability case.

A similar consistent behavior between SR CC and unitary results holds for the other two quantum superpositions, QS2 and QS3. For propagation starting at QS2, in figure 5 we can note the excellent agreement for the TD dipole and probabilities. QS2 is a 50 %-50 % combination of the last two excited states, Ψ_7 and Ψ_8 . Ψ_7 is dominated by the 5th and 7th configurations, whereas Ψ_8 is dominated by the 8th configuration; these are doubles determinants. In figure 5.a we observe that the oscillating patterns of the dipole change after the external field is turned off. Even though the field is on for a short period time, this range of time (0 – 5 fs) is sufficient to drive the eigenstate TD probabilities in a non-trivial fashion, as evidenced in figure 5, where a strong population change occurs. Simulations where the external field is deactivated at longer times were also explored in our present studies without noticing differences in deviations with respect to those presented in this section. On the other hand, the coherence term $p_{wf,78} = C_7^*(t)C_8(t)$ is also described with a striking agreement by the CC operator $\hat{\mathcal{P}}_{78}$ in conjunction with equation (38), figure 5.c. These results suggest the SR formalism offers a promising theoretical method to propagate quantum superpositions while preserving connectedness of quantum mechanical expressions, a condition required to approach macroscopic/periodic systems; where our developments, besides expanding Ref. [68] with the compact inclusion of general quantum superpositions, also provide tools to explore non-diagonal elements of the quantum mechanical density matrix, which depends on an operator such as $\hat{\mathcal{P}}_{IJ}$.

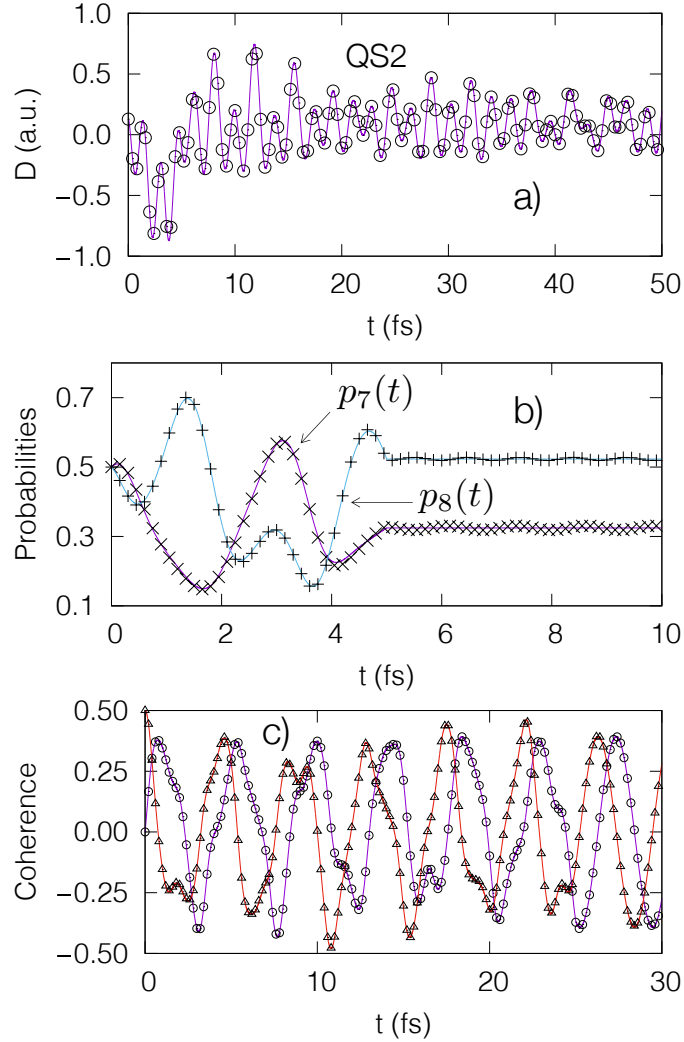


Figure 5. Propagation initiating at the QS2 state. a), TD dipole of the system. Purple line denotes the unitary reference simulation, open circles refer to the SR theory results. b), TD populations of eigenstates Ψ_7 (purple line: exact result, cross symbol: SR simulation) and Ψ_8 (blue line: unitary reference result, “+” symbol: SR theory). c), Coherence of states 7 and 8 (or $p_{78}(t)$) as a function of time; red line: exact result for the real part of this coherence, open triangle: SR theory for the real part; purple line: exact result for imaginary component, open circle: SR theory for this imaginary part.

In our simulations, the operator $\hat{\mathcal{P}}_{IJ}$ was expressed in matrix form by explicitly computing the exponential matrices involved. The resulting matrix was treated as a matrix associated to an observable, which was then symmetrized. In more practical settings, however, computationally efficient ways to use the operator $\hat{\mathcal{P}}_{IJ}$ would be needed. This can be carried out by examining the expressions that result from inserting this operator in equation 12, where a considerable aspect to address in future work concerns truncation of the exponential operators. Furthermore, the symmetrization step is not unique, as expected, as other procedures are possible, and the trace is not strictly the unity if the exponential operator is computed as a truncated power series;

otherwise the approach is norm-conserving. In a unitary version of SR CC, however, this issue may not arise.

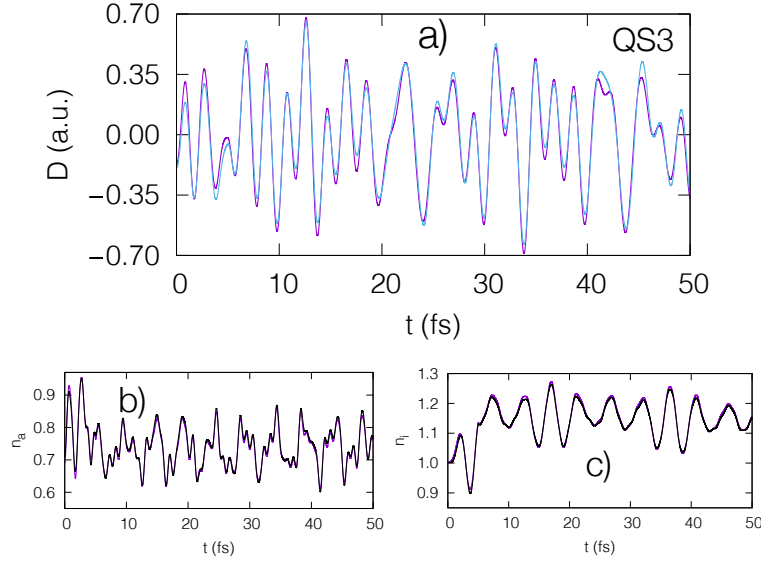


Figure 6. Effect of regularization on dipole and population evolution, starting from QS3. a), TD dipole where the purple and blue lines refer to the numerically exact and the *regularized* SR theory results, respectively. b) and c) show the comparison between the regularized (black line) and unitary (purple line) reference for levels *a* and *i*, correspondingly.

Our SR CC theory results provide support for equation (36), which describes the evolution of a quantum mechanical observable. To further test equation (36), we now examine the response of states that derive from the regularized ground state and the diagonalization of $\tilde{\mathcal{A}}$. Our regularization technique approximates energies and CC vectors, and thereby the associated TD observables. However, it can provide useful results to analyze and understand quantum mechanical quantities. We examine here the case where α is relatively large (compared to $\Delta\epsilon$), $\alpha = 4.0$ eV. For the iterative calculation of the t -amplitudes, in the quasi-Newton step, which involves energy differences in a series of denominators, the regularization number broadens such energy differences by its value, for example, $\epsilon_a - \epsilon_i + \alpha$, and any other energy difference between the configurations. So if the gap between virtual and occupied levels is relatively small, the regularization removes potential instabilities and yields convergent, approximate t , Λ amplitudes. Tables S1 and S2 (supplemental material) show the regularized and exact energy values for the system considered in figure 1. We note that with greater regularization values, the errors increase slightly. The errors, have an upper bound because the larger the α number is, the more negligible the resulting \hat{T} and $\hat{\Lambda}$ vectors become. Nonetheless, there are elements in our theory to improve (not explored in this work) the accuracy of a regularized method. Regularization, in our opinion, is convenient for cases where instabilities arise in the determination of the ground-state cluster amplitudes. To study the response of the system after the ground-state

regularized amplitudes are found, we follow the same steps as for the unregularized propagations discussed before. Figure 6 shows the evolution of the observable \hat{D} for the regularized system with $\alpha = 4.0$ eV. The system in this case begins from the state QS3. As opposed to the unregularized calculations, small deviations are slightly more noticeable in this case due to the effect of the regularization. This can be observed for the dipole, figure 6.a, and the populations of the a and i levels, figures 6.b and .c, respectively. Such deviations are caused by fluctuations in the excitation energies with respect to the exact ones, and in the EOM-CC wavefunctions.

As mentioned in Ref. [68], the present SR CC approach is asymmetric and, *in its current form*, is unable to reproduce *exactly* the standard wavefunction theory results, despite these agree strikingly well. Nonetheless, the robustness of the non-Hermitian SR CC model holds even if the strength of the electron-electron interaction is increased, as shown in figure S1 (supplemental material). Repeating the steps outlined in section 5, but now for $b = 0.25$ eV and $w_0 = U_0 = 0.5$ eV, we observe the same kind of overall agreement between the SR theoretical propagation and the unitary reference evolution. The ground-state amplitudes are in this scenario in the range $[0.08 - 0.2]$, reflecting a strong electron-electron interaction (Tables S3 and S4, supplemental material). Similarly, the regularization method yields the TD quantum dipole in close agreement with both the unregularized SR and standard quantum mechanical results. Deviations with respect to standard simulations occur in our theory because the SR CC wavefunctions display a type of normalization that does not take place in the parent quantum mechanical theory. Even though one can normalize wavefunctions in a form that complies with the Hermitian theory, this would require numerical operations that work against the practical purpose of asymmetric CC theories. However, the unitary CC method is an alternative to the non-Hermitian CC theory that is widely applied in quantum algorithms for simulations in chemistry. The SR theory is applicable to expand TD unitary CC theory, but it necessitates a separate careful analysis not covered in this work. Nonetheless, the present SR theory captures accurately the TD behavior of the observable represented by \hat{A} .

Returning to potential applications of the SR CC theory in realistic cases, for strong external perturbations that are turned on for long enough such that they induce a significant response by the quantum system, high-order excitation vectors of fourth order or beyond could be necessary. In these situations, an alternative approach to avoid such high-order excitation vectors is the use of TD relaxed orbitals [49, 81, 82]. For example, a possibility to expand the SR formalism in this direction is to employ auxiliary reference TD orbitals that derive from a TD variational method. Such orbitals could also be treated as functions of the parameters g_L and g_R . These would in turn provide a basis to find a different set of TD equations for the excitation vectors that may be truncated at the third or second order.

Our proposed SR CC theory derives from the standard (non-Hermitian yet size-extensive) TD CC formalism [32], so it can propagate initial states described by linear quantum superpositions. In practical TD propagations, SR CC methods might inherit

the numerical challenging technicalities of standard TD CC, which arise from its non-linear dependencies on the standard TD excitation vectors. TD EOM-CC theory, in contrast, offers a more direct approach to propagations that does not rely on the non-linear aspects of standard TD CC methods, but it is not size-extensive; TD EOM-CC operates similarly as TD configuration-interaction theory [58, 62]. On the other hand, the non-Hermiticity of standard TD CC [74] has the undesirable issue of breaking strict time-reversibility, which is a fundamental physical constraint, but, as mentioned before, it is a matter that can be resolved in unitary CC theories, or lessened with an external symmetrization [83]. Finally, the starting (initial-state) transition elements in our theory requires, in principle, the application of conventional response theory, which can be computationally demanding for large systems, but still remains size extensive. For simplicity we expressed these elements in a sum-over-states fashion, which requires EOM-CC eigenvectors and eigenvalues, but evidences the fact that these can be computationally expensive. However, approximations or approaches that circumvent the need for response-theory relaxation terms for initial observable matrices, such as dipole matrices, could improve computational efficiency and be the subject of future work.

7. Conclusion

This work examines in depth second response theory, a time-dependent coupled-cluster formalism to propagate general quantum superpositions, and presents a simple formula, not developed previously, that predicts accurately the evolution of a quantum mechanical observable of interest, including probabilities and coherences. Our theory gives connected expressions to determine observables in the non-linear regime, and requires the solution to the standard ground-state propagation problem and the time-dependency of three response excitation vectors. With these elements provided, we studied its application to a model three-electron/three-level system under different initial quantum superpositions. This type of propagation is relevant to further developing theoretical approaches and the study of systems that are thermally and/or optically excited. Finally, we examined the use of the SR energy expressions to approach regularized systems, which do not solve exactly the ground-state problem, but offer stable approximations to its cluster amplitudes, excited-state energies, and CC excitation vectors. These could lead to further improvements to cases where determining the cluster amplitudes is difficult because of low energy gaps, or related adverse effects.

Acknowledgments

M.A.M. thanks Montana State University, Bozeman, for startup funding. The author also acknowledges support by the National Science Foundation through the MonArk Quantum Foundry, DMR-1906383.

References

- [1] Marzari N, Ferretti A and Wolverton C 2021 *Nat. Mater.* **20** 736–749
- [2] Morton S M, Silverstein D W and Jensen L 2011 *Chem. Rev.* **111** 3962–3994
- [3] Xie C, Yan D, Chen W, Zou Y, Chen R, Zang S, Wang Y, Yao X and Wang S 2019 *Mater. Today* **31** 47–68
- [4] Cao Y, Romero J, Olson J P, Degroote M, Johnson P D, Kieferová M, Kivlichan I D, Menke T, Peropadre B, Sawaya N P *et al.* 2019 *Chem. Rev.* **119** 10856–10915
- [5] McArdle S, Endo S, Aspuru-Guzik A, Benjamin S C and Yuan X 2020 *Rev. Mod. Phys.* **92** 015003
- [6] Bauer B, Bravyi S, Motta M and Chan G K L 2020 *Chem. Rev.* **120** 12685–12717
- [7] Kökcü E, Steckmann T, Wang Y, Freericks J, Dumitrescu E F and Kemper A F 2022 *Phys. Rev. Lett.* **129** 070501
- [8] Motta M and Rice J E 2022 *WIREs Comput. Mol. Sci.* **12** e1580
- [9] Raha K, Peters M B, Wang B, Yu N, Wollacott A M, Westerhoff L M and Merz Jr K M 2007 *Drug Discov. Today* **12** 725–731
- [10] Cavalli A, Carloni P and Recanatini M 2006 *Chem. Rev.* **106** 3497–3519
- [11] Saal J E, Kirklin S, Aykol M, Meredig B and Wolverton C 2013 *JOM* **65** 1501–1509
- [12] Greeley J, Jaramillo T F, Bonde J, Chorkendorff I and Nørskov J K 2006 *Nat. Mater.* **5** 909–913
- [13] van der Kamp M W and Mulholland A J 2013 *Biochem.* **52** 2708–2728
- [14] Jones L O, Mosquera M A, Schatz G C and Ratner M A 2020 *J. Am. Chem. Soc.* **142** 3281–3295
- [15] Baskes M I 1992 *Phys. Rev. B* **46** 2727
- [16] Lachance-Quirion D, Tabuchi Y, Gloppe A, Usami K and Nakamura Y 2019 *Appl. Phys. Express* **12** 070101
- [17] Provorse M R and Isborn C M 2016 *Int. J. Quantum Chem.* **116** 739–749
- [18] Wang Z, Peyton B G and Crawford T D 2022 *J. Chem. Theory Comput.* **18** 5479–5491
- [19] Palacios A and Martín F 2020 *WIREs Comput. Mol. Sci.* **10** e1430
- [20] Samanta P K, Mukherjee D, Hanauer M and Köhn A 2014 *J. Chem. Phys.* **140** 134108
- [21] Dral P O and Barbatti M 2021 *Nat. Rev. Chem.* **5** 388–405
- [22] Park J W, Al-Saadon R, MacLeod M K, Shiozaki T and Vlasisavljevich B 2020 *Chem. Rev.* **120** 5878–5909
- [23] Austin B M, Zubarev D Y and Lester Jr W A 2012 *Chem. Rev.* **112** 263–288
- [24] Vitillo J G, Cramer C J and Gagliardi L 2022 *Isr. J. Chem.* **62** e202100136
- [25] von Lilienfeld O A, Müller K R and Tkatchenko A 2020 *Nat. Rev. Chem.* **4** 347–358
- [26] Sneskov K and Christiansen O 2012 *WIREs Comput. Mol. Sci.* **2** 566–584
- [27] Zhang I Y and Grüneis A 2019 *Front. Mater.* **6** 123
- [28] Liu J and Cheng L 2021 *WIREs Comput. Mol. Sci.* **11** e1536
- [29] Bartlett R J and Purvis G D 1978 *Int. J. Quantum Chem.* **14** 561–581
- [30] Paldus J 1994 *Algebraic approach to coupled cluster theory* (Boston, MA: Springer US) pp 207–282
- [31] Bartlett R J 2012 *WIREs Comput. Mol. Sci.* **2** 126–138
- [32] Koch H and Jørgensen P 1990 *J. Chem. Phys.* **93** 3333–3344
- [33] Bartlett R J and Musiał M 2007 *Rev. Mod. Phys.* **79** 291–352
- [34] Taube A G and Bartlett R J 2009 *J. Chem. Phys.* **130** 144112
- [35] Shen Y, Zhang X, Zhang S, Zhang J N, Yung M H and Kim K 2017 *Phys. Rev. A* **95** 020501
- [36] Harsha G, Shiozaki T and Scuseria G E 2018 *J. Chem. Phys.* **148** 044107
- [37] Lee J, Huggins W J, Head-Gordon M and Whaley K B 2018 *J. Chem. Theory Comput.* **15** 311–324
- [38] Evangelista F A, Chan G K and Scuseria G E 2019 *J. Chem. Phys.* **151** 244112
- [39] Romero J, Babbush R, McClean J R, Hempel C, Love P J and Aspuru-Guzik A 2018 *Quantum Sci. Technol.* **4** 014008
- [40] Xia R and Kais S 2020 *Quantum Sci. Technol.* **6** 015001
- [41] Ryabinkin I G, Yen T C, Genin S N and Izmaylov A F 2018 *J. Chem. Theory Comput.* **14** 6317–6326

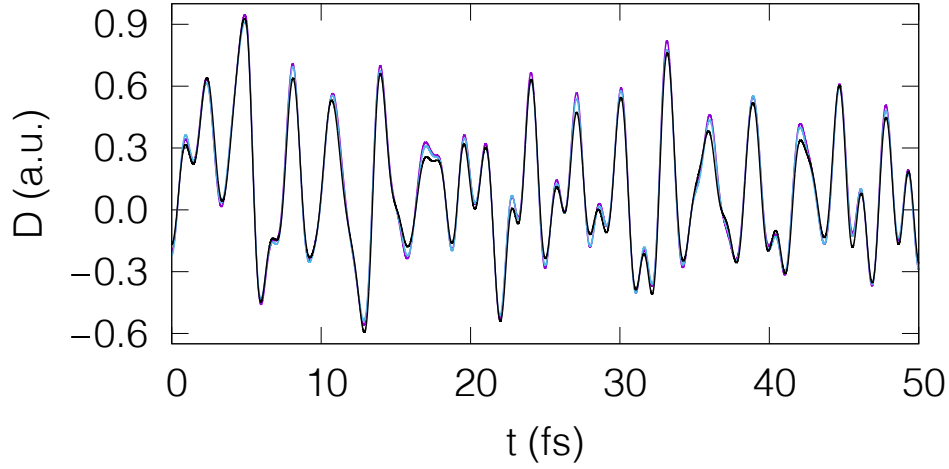
- [42] Anand A, Schleich P, Alperin-Lea S, Jensen P W, Sim S, Díaz-Tinoco M, Kottmann J S, Degroote M, Izmaylov A F and Aspuru-Guzik A 2022 *Chem. Soc. Rev.* **51** 1659–1684
- [43] Neufeld V A, Ye H Z and Berkelbach T C 2022 *J. Phys. Chem. Lett.* **13** 7497–7503
- [44] Wang X and Berkelbach T C 2021 *J. Chem. Theor. Comput.* **17** 6387–6394
- [45] Folkestad S D, Sannes B S and Koch H 2023 *The Journal of Chemical Physics* **158**
- [46] Ofstad B S, Aurbakken E, Schøyen Ø S, Kristiansen H E, Kvaal S and Pedersen T B 2023 *WIREs Comput. Mol. Sci.* e1666
- [47] Skeidsvoll A S, Moitra T, Balbi A, Paul A C, Coriani S and Koch H 2022 *Physical Review A* **105** 023103
- [48] Pathak H, Sato T and Ishikawa K L 2022 *Front. Chem.* **10** 982120
- [49] Pathak H, Sato T and Ishikawa K L 2021 *J. Chem. Phys.* **154** 234104
- [50] Skeidsvoll A S, Balbi A and Koch H 2020 *Phys. Rev. A* **102** 023115
- [51] Pedersen T B, Kristiansen H E, Bodenstern T, Kvaal S and Schøyen Ø S 2020 *J. Chem. Theory Comput.* **17** 388–404
- [52] Pedersen T B and Kvaal S 2019 *J. Chem. Phys.* **150** 144106
- [53] Koulias L N, Williams-Young D B, Nascimento D R, DePrince III A E and Li X 2019 *J. Chem. Theory Comput.* **15** 6617–6624
- [54] White A F and Chan G K L 2019 *J. Chem. Theory Comput.* **15** 6137–6153
- [55] White A F and Chan G K L 2018 *J. Chem. Theory Comput.* **14** 5690–5700
- [56] Park Y C, Perera A and Bartlett R J 2019 *J. Chem. Phys.* **151** 164117
- [57] Nascimento D R and DePrince III A E 2017 *J. Phys. Chem. Lett.* **8** 2951–2957
- [58] Nascimento D R and DePrince III A E 2016 *J. Chem. Theor. Comput.* **12** 5834–5840
- [59] Pigg D A, Hagen G, Nam H and Papenbrock T 2012 *Phys. Rev. C* **86** 014308
- [60] Wälz G, Kats D, Usvyat D, Korona T and Schütz M 2012 *Phys. Rev. A* **86** 052519
- [61] Kats D, Usvyat D and Schütz M 2011 *Phys. Rev. A* **83** 062503
- [62] Sonk J A, Caricato M and Schlegel H B 2011 *The Journal of Physical Chemistry A* **115** 4678–4690
- [63] Monkhorst H J 1977 *Int. J. Quantum Chem.* **12** 421–432
- [64] Schönhammer K and Gunnarsson O 1978 *Phys. Rev. B* **18** 6606
- [65] Hoodbhoy P and Negele J 1978 *Phys. Rev. C* **18** 2380
- [66] Hoodbhoy P and Negele J 1979 *Phys. Rev. C* **19** 1971
- [67] Arponen J 1983 *Ann. Phys.–New York* **151** 311–382
- [68] Mosquera M A 2022 *Phys. Rev. A* **106** 052805
- [69] Mosquera M A, Chen L X, Ratner M A and Schatz G C 2016 *J. Chem. Phys.* **144** 204105
- [70] Mosquera M A, Jackson N E, Fauvell T J, Kelley M S, Chen L X, Schatz G C and Ratner M A 2017 *J. Am. Chem. Soc.* **139** 3728–3735
- [71] Mosquera M A, Jones L O, Kang G, Ratner M A and Schatz G C 2021 *J. Phys. Chem. A* **125** 1093–1102
- [72] Helgaker T, Jørgensen P and Olsen J 2014 *Molecular electronic-structure theory* (John Wiley & Sons)
- [73] Stanton J F and Bartlett R J 1993 *J. Chem. Phys.* **98** 7029–7039
- [74] Pedersen T B and Koch H 1997 *J. Chem. Phys.* **106** 8059–8072
- [75] Lawler K V, Parkhill J A and Head-Gordon M 2008 *Mol. Phys.* **106** 2309–2324
- [76] Stück D and Head-Gordon M 2013 *J. Chem. Phys.* **139** 5203–5219
- [77] Jacobson G, Marmolejo-Tejada J M and Mosquera M A 2023 *ChemPhysChem* **24** e202200592
- [78] Mosquera M A 2021 *J. Phys. Chem. A* **125** 8751–8763
- [79] Helgaker T and Jørgensen P 1988 *Adv. Quantum Chem.* **19** 183–245
- [80] Helgaker T, Jørgensen P and Handy N C 1989 *Theor. Chim. Acta* **76** 227–245
- [81] Kvaal S 2012 *J. Chem. Phys.* **136** 194109
- [82] Sato T, Pathak H, Orimo Y and Ishikawa K L 2018 *J. Chem. Phys.* **148** 051101
- [83] Pedersen T B and Koch H 1998 *J. Chem. Phys.* **108** 5194–5204

Supplemental material. Second response theory: A theoretical formalism for the propagation of quantum superpositions

Martín A. Mosquera

Department of Chemistry and Biochemistry, Montana State University, Bozeman,
MT 59718, USA

E-mail: martinmosquera@montana.edu



$$\Psi(0) = \sum_{N=0,1,2} \frac{1}{\sqrt{3}} \Psi_N \quad \begin{aligned} b &= 0.25 \text{ eV} \\ w_0 = U_0 &= 0.5 \text{ eV} \end{aligned}$$

Figure S1. Evolution remains robust upon increasing the electron-electron interaction strength. Purple line: exact result, blue line: SR theory (no regularization), black line: regularized SR results ($\alpha = 4.0$ eV).

1. Extra equations

The TD cluster operators $\hat{\lambda}_r^E$, $\hat{\lambda}_l^E$, and $\hat{\lambda}_{l,r}^E$ follow the relations:

$$-i\partial_t \lambda_{l,\mu}^E(t) = \langle \hat{\lambda}_l^E(t) [\bar{H}_x(t), \hat{\tau}_\mu] \rangle_0, \quad (\text{S1})$$

$$-i\partial_t \lambda_{r,\mu}^E(t) = \langle \hat{\lambda}(t) [\bar{H}_{x,\tau,\mu}(t), \hat{x}_r(t)] + \hat{\lambda}_r^E(t) \bar{H}_{x,\tau,\mu}(t) \rangle_0, \quad (\text{S2})$$

$$-i\partial_t \lambda_{l,r,\mu}^E(t) = \langle \hat{\lambda}_{l,r}^E(t) \bar{H}_{x,\tau,\mu}(t) + \hat{\lambda}_l^E(t) [\bar{H}_{x,\tau,\mu}(t), \hat{x}_r(t)] \rangle_0. \quad (\text{S3})$$

2. Tables

Table S1. Energies the eigen-states of the unperturbed 3-electron/3-level system for the case where b , w_0 and U_0 are 0.1, 0.2, and 0.2 eV, respectively. For each state we show the most dominant configurations (Figure 1). We denote the dominant configurations simply as “Config.” below. For example, wavefunction (WF) Ψ_3 is dominated by the 6th and 2nd configurations. We also show the effect of regularization for three different values of α , 0.5, 4.0, and 8.0 eV.

WF No.	Energy (a.u.)	Config.	E_N , $\alpha = 0.5$ eV	E_N , $\alpha = 4.0$ eV	E_N , $\alpha = 8.0$ eV
0	0.03406112	0	0.03450364	0.03567967	0.03607546
1	0.07313581	1	0.07321405	0.07338131	0.07342816
2	0.08035159	3	0.08047917	0.08070788	0.08076523
3	0.10975262	6, 2	0.10986812	0.11009739	0.11015831
4	0.10994818	2, 6	0.11002712	0.11016849	0.11020221
5	0.11190407	4	0.11153361	0.11076561	0.11055775
6	0.15482654	7, 5	0.15471626	0.15449552	0.15443684
7	0.15583540	5, 7	0.15558061	0.15493385	0.15471786
8	0.19183032	8	0.19172308	0.19141593	0.19130383

Table S2. Ground-state cluster amplitudes ($\{t_\mu\}$) of the 3-electron/3-level system for the case where b , w_0 and U_0 are 0.1, 0.2, and 0.2 eV, respectively. We also show the effect of regularization on these amplitudes for three different values of α , 0.5, 4.0, and 8.0 eV.

Configuration	t_μ (unitless)	t'_μ , $\alpha = 0.5$ eV	t'_μ , $\alpha = 4.0$ eV	t'_μ , $\alpha = 8.0$ eV
1	-0.07950747	-0.05601643	-0.01868837	-0.01067200
2	-0.04329081	-0.03546118	-0.01573367	-0.00964238
3	-0.06698762	-0.04964707	-0.01797352	-0.01044045
4	-0.09473071	-0.07728911	-0.03312300	-0.01995302
5	-0.06063376	-0.05290738	-0.02763888	-0.01782138
6	-0.04330929	-0.03546662	-0.01573373	-0.00964238
7	-0.06079416	-0.05299412	-0.02764646	-0.01782314
8	-0.04665203	-0.04190695	-0.02428942	-0.01636484

Table S3. Energies of the eigen-states of the unperturbed 3-electron/3-level system for the case where b , w_0 and U_0 are 0.25, 0.5, and 0.5 eV, respectively. For each state we show the most dominant configurations (Figure 1). We denote the dominant configurations simply as “Config.” below. For example, Ψ_7 is dominated by the 5th and 7th configurations. We also show the effect of regularization for three different values of α , 0.5, 4.0, and 8.0 eV.

WF No.	Energy (a.u.)	Config.	E_N , $\alpha = 0.5$ eV	E_N , $\alpha = 4.0$ eV	E_N , $\alpha = 8.0$ eV
0	0.0236728	0	0.02523072	0.03055085	0.03271333
1	0.0704724	1	0.07096318	0.07230300	0.07275556
2	0.0877195	3	0.08833656	0.09007605	0.09071326
3	0.1074657	6, 2	0.10792629	0.10915896	0.10957066
4	0.1088416	2, 6	0.10907914	0.10971073	0.10991757
5	0.1193940	4	0.11809707	0.11421255	0.11277842
6	0.1678397	7, 5	0.16744433	0.16635852	0.16598905
7	0.1733486	5, 7	0.17234761	0.16909455	0.16779473
8	0.2069911	8	0.20632056	0.20428027	0.20351289

Table S4. Ground-state cluster amplitudes ($\{t_\mu\}$) of the 3-electron/3-level system for the case where b , w_0 and U_0 are 0.25, 0.5, and 0.5 eV, respectively. We also show the effect of regularization on these amplitudes for three different values of α , 0.5, 4.0, and 8.0 eV.

Configuration	t_μ (unitless)	t'_μ , $\alpha = 0.5$ eV	t'_μ , $\alpha = 4.0$ eV	t'_μ , $\alpha = 8.0$ eV
1	-0.12821361	-0.10064334	-0.04148473	-0.02494136
2	-0.08356321	-0.07146805	-0.03567552	-0.02271260
3	-0.09336382	-0.07877364	-0.03782335	-0.02364346
4	-0.20069546	-0.17111214	-0.08042701	-0.04931169
5	-0.12600387	-0.11349122	-0.06485739	-0.04297576
6	-0.08380465	-0.07156498	-0.03567760	-0.02271279
7	-0.12667178	-0.11397311	-0.06493685	-0.04299760
8	-0.10135496	-0.09296701	-0.05748125	-0.03959413